

Experimental and theoretical description of the plastic behaviour of semicrystalline polymers

G. Spathis* and E. Kontou

*Department of Engineering Science, Section of Mechanics,
National Technical University of Athens, 5 Heroes of Polytechnion,
GR-15773, Athens, Greece
(Received 4 November 1996; revised 20 January 1997)*

In this work, a new experimental technique, based on a non-contact method of strain measurement, has been applied in the case of semicrystalline polymers, where yielding occurs through inhomogeneous deformation (necking). It was then possible to construct the true stress–strain curves at various crosshead speeds tested. Furthermore, a constitutive model for the description of this behaviour has been introduced, grounded on a plasticity theory, which has been developed and initially applied on plastic behaviour of crystalline metals. This theoretical model was proved to predict satisfactorily the experimental results. Moreover, the rate effect and the post yield phenomena, as possible strain softening and strain hardening have also been described in terms of molecular parameters connected with the material tested. © 1997 Elsevier Science Ltd.

(Keywords: plastic behaviour; semicrystalline polymers)

INTRODUCTION

Semicrystalline polymers are essentially composite materials with alternating crystalline and non-crystalline regions. The basic structural element associated with the crystalline phase is the unit cell of the polymeric single crystal, while the structural element of the non-crystalline phase is viewed as a collection of macromolecular chain segments, not included in the crystal structure^{1,2}.

Each structural element has its own properties, resulting from the molecular interactions between the polymer chains. Due to the fact that the interactions along molecular chains differ to those across their axis, the resulting properties of each structural element are anisotropic.

The mechanical properties of the structural element can be described by using the compliance or elastic constants tensor. In the case of transversely isotropic symmetry, five independent constants are required. It is expected that the mechanical properties of the polymer will depend on both the crystalline morphology and molecular orientation of the structural element. It has been proposed that the polymer can be regarded as an aggregate of these anisotropic elastic units, whose properties are those of the highly oriented fibre of polymer^{3,4}. By averaging the compliance constants, the elastic properties of isotropic aggregate are defined, called 'Reuss average'⁵, while by averaging the stiffness constants, the elastic properties of the isotropic aggregate, called Voigt average⁶, are the results.

When the isotropic specimen is then uniaxially stretched, the aggregate model can be extended to determine the mechanical anisotropy as a function of the draw ratio.

On the other hand, the material behaviour of amorphous glassy as well as semicrystalline polymers, after an initial elastic response, is not yet well characterized. The yield mechanism and post-yield behaviour exhibit several distinct features. The initial yielding of the material is known to depend on pressure, strain rate and temperature. The

description of yielding can be made by different approaches. One of them is based on a possible analogy with plasticity of nonpolymeric materials. It is assumed that the yield point results from the initiation and propagation of defects of the type of dislocation⁷. Another approach assumes that yielding in polymers is related to molecular relaxation processes, occurring when the plastic flow rate is equal to the applied strain rate. After yielding, the polymeric material may possess the response of true strain softening. Especially in semicrystalline polymers, the yielding and cold-drawing deformation contain two types of non-uniform deformation processes: one is the initiation of local necking and the other is the propagation of necking shoulders along the specimen. Both types are due to the local instability of deformation, but they are different in behaviour⁸. Hereafter, as larger strains are approached, the material hardens.

This aspect is a consequence of the orientation of the polymer molecules and relates generally to the effects of conformation and orientation on mechanical properties. The molecular alignment alters the configurational entropy of the material, and can be represented by a Gaussian or Langevin equation^{9–11}.

The mathematical formulation for constructing constitutive models which take into account all those characteristics of semicrystalline polymers is a hard and particular task, given that combination of mechanical anisotropy developed during plastic flow with inhomogeneous deformation (necking instability) lacks complete theoretical account. In spite of the fact that a large number of works have dealt with elastic–plastic behaviour of polycrystalline solids, it has not yet been completely characterized.

In this work, an attempt will be made to develop a constitutive model based on the macromolecular structure of semicrystalline materials and the micromechanism of plastic flow. The present analysis is based on a theory for elastic–plastic material, which is valid for general anisotropic response and is independent of the choice of reference configuration from which the total strain is measured. More

* To whom correspondence should be addressed

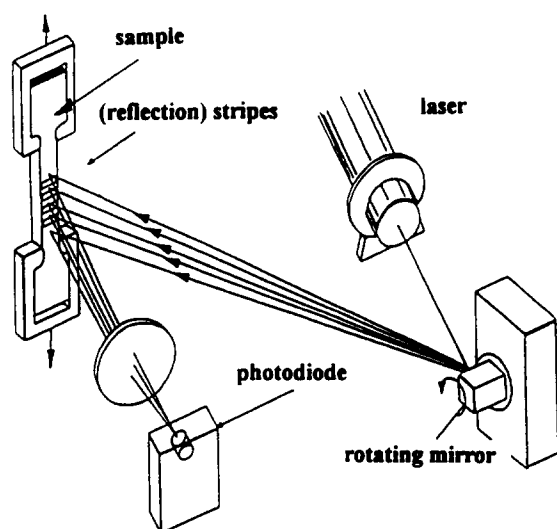


Figure 1 Schematic presentation of the principle of the Laser Extensometer

specifically, in this treatment, the theoretical work developed by Rubin^{12,13} for the plastic description of crystalline metals will be used.

His approach has been adapted for the case of semicrystalline polymers, by assuming that the structural elements, during the test procedure, change orientation, retaining their size and elastic constants unaffected.

According to Rubin's treatment, an evolution equation for elastic deformation has been defined without specifying a plastic deformation tensor explicitly. This can be made by introducing a vector triad \mathbf{m}_i , which models the orientation and elastic deformation of the crystalline regions.

The validity of the proposed treatment has been tested by tensile testing of a widely used semicrystalline polymer, polypropylene. Generally, the load–elongation data transformed into engineering stress–strain curves, do not provide a correct description of the mechanical behaviour of the material, which requires the measurement of the true stress and true strain in local terms¹¹. The intrinsic response of the material tested has been assessed by means of a new experimental technique.

The used system permits a non-contact measurement of longitudinal deformation distribution of the specimen, while the load is recorded simultaneously. For a constant cross-head speed experiment it has been found that the local strain

rate appears to vary by one or two orders of magnitude. Therefore, the tensile stress had to be corrected for this strain rate variation, assuming that the deformation procedure is isovolume. In this way, the true tensile stress–strain curves have been constructed at three different cross-head speeds tested.

The theoretical description of these curves has been made successfully. It must be noted that the parameters used in the numerical evaluation of the related equations constitute elastic constants of the crystalline phase of polypropylene and have been established in the literature. The rest of the parameters required are not curve fitting constants, but they are grounded on a physical base connected with molecular features.

MATERIALS–EXPERIMENTAL PROCEDURE

The polypropylene used in the present work is produced under the commercial reference APPRYL 3020 BNI, with a melt index equal to 1.9 g/min. It was processed in the shape of cylindrical extruded rods, 3.5 mm in diameter and exempt of bubbles. Dogbone tensile specimens have then been constructed with an average thickness of 3 mm and a gauge length of 30 mm.

The tensile experiments have been carried out with an Instron 1121 tester at room temperature. Three different cross-head speeds have been used, i.e. 0.1, 1 and 10 mm/min. The longitudinal strain could be measured very accurately with the LaserExtensometer, which permits a non-contact measurement of the longitudinal deformation distribution of samples.

The system is constructed according to the principle of *Figure 1*. A beam is cast by a laser onto a rotating mirror. By rotation of the mirror, the laser scans a tape pattern code which is applied on the specimen. A special painting technique has been followed for the application of a deformable coating on the sample. The reflections of the tape patterns are registered by a photocell. The part of the sample to be measured is determined and limited by the opening in the case, as shown in *Figure 2*. Due to the geometric arrangements, the aperture θ is approximately 23° . During rotating of the mirror and before leaving the case, the laser beam slips over the first photodiode that gives a start signal. After scanning, a stop signal is given by the second photodiode.

For the elongation measurements, a contrasting tape pattern code was applied to the gauge length of the sample,

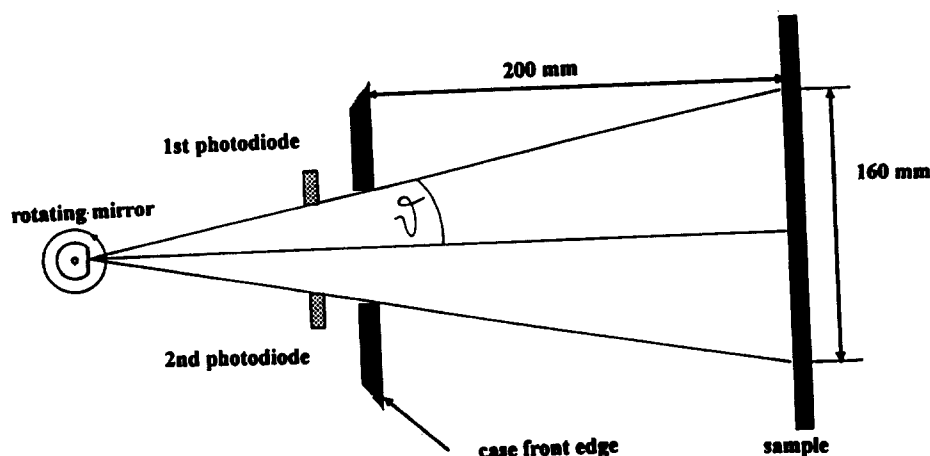


Figure 2 Measuring geometry of the test system

i.e. 15 white stripes on dark ground. The space between stripes was 1 mm. From the gap between the first and the last marking and the mirror speed, the calibration of the path length results as the middle value of the first scans. For a scanning, 36 ms are needed irrespective of the samples length. At the beginning (and end) of the scan, a start (stop) signal is given. The actual elongation measurement is done via counting units. In case a reflection of the sample marking reaches the detector during the counting process, the actual counter count is buffered and the position of the stripes is determined. The total time needed for recording an elongation experiment depends on the number of memories, scan speed and number of marking lines applied.

During the tensile test the load was recorded simultaneously with the percentage strain, and the data acquisition has been made with software. The construction of engineering and true stress-strain curve was then made, as will be discussed below.

EXPERIMENTAL RESULTS

The validity of various models is widely checked by tensile testing, where the load-elongation data are transformed into engineering stress-strain curves, which, however, do not provide a correct description of the mechanical behaviour of the materials. Especially, the behaviour of semicrystalline polymeric materials in a tensile test is more complicated than for a typical amorphous polymer, because its originally isotropic elastic behaviour is followed by an anisotropic elastoplastic response. The yielding and cold-drawing deformation of semicrystalline polymers contain two types of nonuniform deformation process: one is the initiation of local necking and the other is the propagation of necking shoulders along the specimen. Therefore, in order to have access to the objective intrinsic response of the material, the true stress-strain curve is required.

The experimental method used in the present work as mentioned above, has the advantage of giving a detailed description of the deformation distribution, as well as the corresponding strain rates along the gauge length of the material tested.

The time evolution of strain distributed along 10 successive zones, numbering from zone number 4 to zone number 13, of the specimen gauge length is shown in Figure 3. These 10 zones have been selected as equally spaced around the region where yield initiation takes place.

As observed, during the initial elastic response all zones have almost the same strain. Hereafter, when yielding

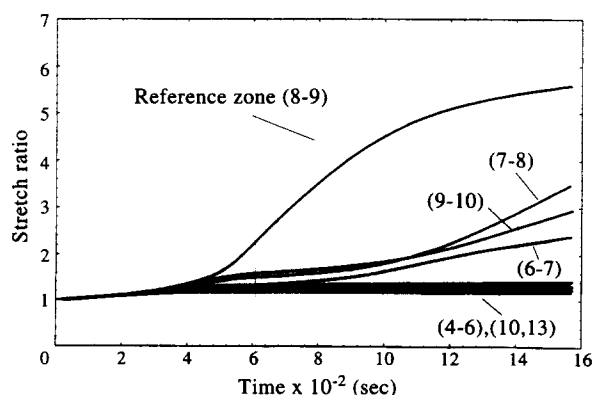


Figure 3 Strain variation versus time between 10 successive zones, each of length 1 mm, along the specimen gauge length

occurs followed by necking initiation at a specific zone, a large deviation of strain appears in respect to the rest regions, where a small decrease of strain takes place.

This deviation appears to have a decremental trend when the neck propagation has completely gone through this specific zone, extending into the neighbored regions. Apart from the fact that the test has been performed at constant cross-head speed, the localized strain rates appear to vary by one or two orders of magnitude, and for the case of a cross-head speed of 1 mm/min are plotted in Figure 4, in respect to true strain ε and the true strain rate $\dot{\varepsilon}$ calculated from the following relations:

$$\varepsilon = \ln(1 + e) \quad (1)$$

$$\dot{\varepsilon} = \frac{1}{1 + e} \frac{de}{dt}$$

where e is the engineering strain.

This figure presents the corresponding strain rates of the 10 successive zones. From these plots, it will be seen that the strain rate is initially very slow and almost equal to the imposed strain rate for all zones tested; then, at a specific zone (in our case that between stripes numbered 8 and 9) where necking is initiated (called hereafter reference zone) speeds up, reaching a high peak after which it decreases. At this stage, the above decrement of the strain rate constitutes strong evidence of the development of strain hardening. This effect is a result of molecular alignment and crystalline orientation.

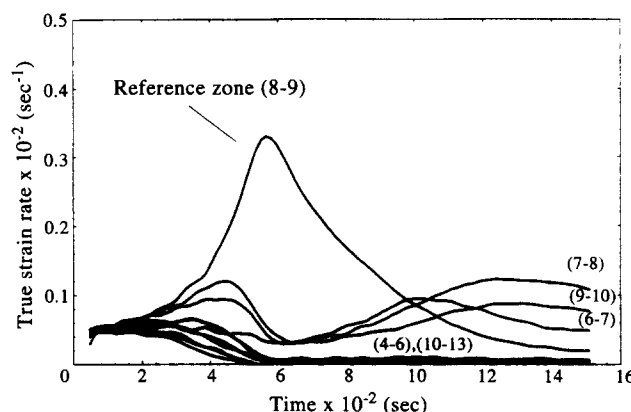


Figure 4 True strain rate variation versus time between 10 successive zones, along the specimen gauge length

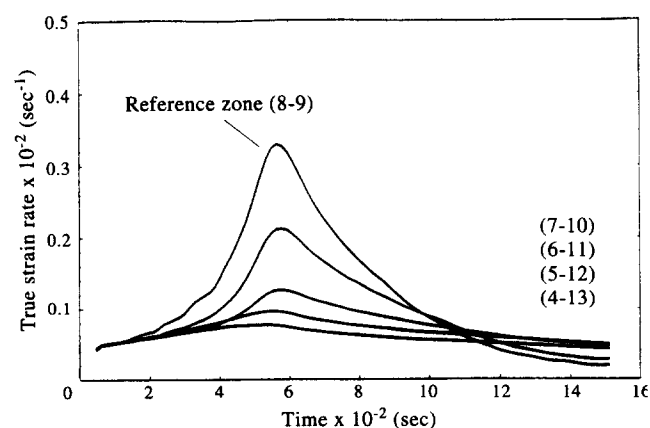


Figure 5 True strain rate versus time of regions including an increasing number of successive zones, starting from the reference one

From Figure 4, it is obvious that the highest strain rate appears in the reference zone which has a gauge length of 1 mm. This length is however still large compared with the real localized plastic region where neck initiation takes place. If we had the possibility to minimize the reference length to the dimension of this localized region, then the respective strain rate would be equal to the plastic rate of deformation Γ_p . In order to approximate this magnitude, a scaling procedure can be established. In Figure 5, plots of strain rates of the various zones, starting from the reference one with the neck initiation and moving equivalently from both sides up to the total specimen gauge length, are presented. By extrapolating this scaling behaviour up to the region where plastic deformation initiates, we can conclude that the rate of plastic deformation Γ_p is given by:

$$\Gamma_p = k \dot{\epsilon}_r \tag{2}$$

where k is an amplification factor, which will be defined below and $\dot{\epsilon}_r$ is the strain rate of the reference zone.

Due to the fact that the major interest of this work is to explain the mechanical response of semicrystalline polymers, the true stress-strain curves should be determined at various strain rates.

Considering the stress σ_a , obtained by dividing the load P by the original cross-sectional area A_0

$$\sigma_a = \frac{P}{A_0} \tag{3}$$

the engineering stress-strain curves are shown in Figure 6 (typical for a cold drawing material) for the cross-head speeds tested. This plot has been made with respect to the

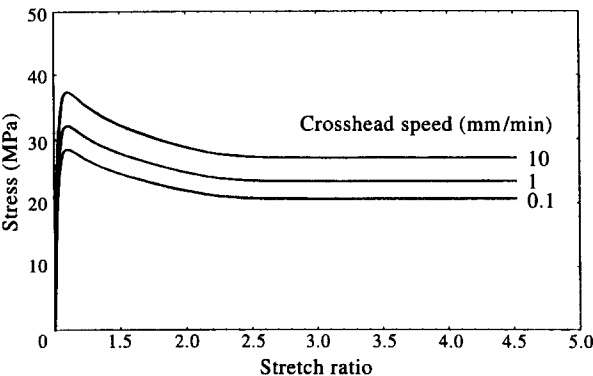


Figure 6 Engineering tensile stress-strain curves of polypropylene at three different cross-head speeds

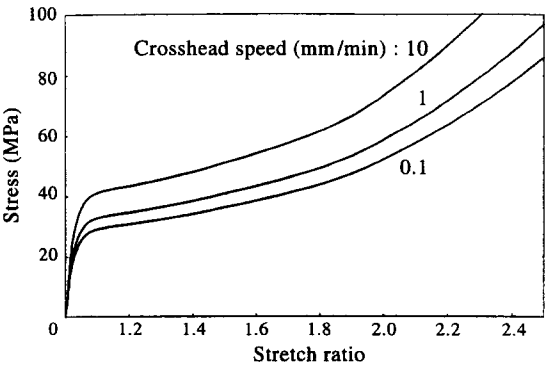


Figure 7 Tensile true stress-strain curves of polypropylene at three different cross-head speeds, plotted with respect to equation (4)

reference zone. As is shown, the load reaches its maximum value when the uniform extension of the sample stops. At this moment, neck initiation takes place and then the load falls, as observed in the last part of the stress-strain curve. Finally, fracture occurs at the narrowest point of the neck.

Due to this nonuniform deformation, it is more informative to plot the true tensile stress-strain curve. Assuming that the deformation procedure takes place under isovolume conditions, this effective stress is:

$$\sigma = \frac{P}{A} = \frac{(1 + e)P}{A_0} = \sigma_a(1 + e) \tag{4}$$

where A is the actual cross-section at any time. The true stress-strain curves for the three cross-head speeds tested are shown in Figure 7. They exhibit the classical shape commonly observed for semicrystalline polymers. The material yields progressively at a strain almost equal to 10%, showing the respective influence of strain rate. No stress drop is observed after the yield point, while at higher strains a subsequent strain hardening takes place.

CONSTITUTIVE EQUATIONS

Due to the fact that yield phenomenon is a main feature in soft metals, a large amount of theoretical work has been developed for the elastic-plastic behaviour of polycrystalline solids. However, the corresponding constitutive equations for large deformations of these materials are still in a state of development. The main differences among the various trends concern the way in which the total deformation gradient tensor \mathbf{F} (which describes the way a material line element $d\mathbf{X}$ deforms in a line element $d\mathbf{x}$ in the present state), is separated into the elastic and plastic parts \mathbf{F}_e and \mathbf{F}_p , correspondingly.

These two tensors lack an explicit determination in the present configuration of the material elements, because each of them is referred to different configurational states.

To avoid this problem, a detailed description has been developed by Rubin^{12,13} who extended the ideas by Eckard¹⁴ and Besseling¹⁵. In this work, an evolution equation for elastic deformation has been specified including the relaxation effects of plastic deformation without introducing a plastic deformation tensor explicitly.

Although Rubin's treatment has been introduced for describing a general anisotropic response of crystalline metals, an attempt will be made here to apply this method in the case of semicrystalline polymers. In what follows, the main features of Rubin's work will be adapted to the special case of the materials tested.

According to his assumption, the elastic deformation of each material point has been formulated through a triad of vectors \mathbf{m}_i , that are related to the dilatation, distortion and orientation of the mean atomic lattice in respect to some reference state.

In the case of semicrystalline polymers, where a large number of crystalline regions is randomly oriented into the amorphous matrix, it may be assumed that vectors \mathbf{m}_i are defined to characterize the deformation state of a large number of such crystalline regions. In the reference configurational state associated with the material, when it is stress-free, this triad of vectors constitutes a set of orthonormal vectors, implying that the corresponding metric tensor m_{ij} equal to $m_{ij} = \mathbf{m}_i \cdot \mathbf{m}_j$ is given by:

$$m_{ij} = \delta_{ij} \tag{5}$$

In order to define the change of the volume element we are referred to, the dilatation J_m (which is unity in the reference lattice state) is introduced and given by:

$$J_m = \mathbf{m}_1 \times (\mathbf{m}_2, \mathbf{m}_3) = (\det \mathbf{m}_{ij})^{1/2} \quad (6)$$

Moreover, to define the distortional measures of the elementary volume, Rubin has introduced another set of orthonormal vectors \mathbf{m}'_i defined by the equations:

$$\mathbf{m}'_i = J_m^{-1/3} \mathbf{m}_i \text{ with } m'_{ij} = \mathbf{m}'_i \cdot \mathbf{m}'_j = J_m^{-2/3} m_{ij} \quad (7)$$

It is easily then extracted that:

$$\det \mathbf{m}'_{ij} = 1 \quad (8)$$

The microstructural variables \mathbf{m}_i are determined by an evolution equation of the form:

$$\dot{\mathbf{m}}_i = \mathbf{L}_m \mathbf{m}_i \quad (9)$$

where the second order tensor \mathbf{L}_m , corresponds to the elastic velocity gradient and is assumed to be separated additively into the form:

$$\mathbf{L}_m = \mathbf{L} - \mathbf{L}_p \quad (10)$$

where \mathbf{L} and \mathbf{L}_p are the velocity gradients of total and plastic deformation, respectively.

Concerning uniaxial stress in the \mathbf{e}_i direction in respect to a fixed rectangular Cartesian base vector \mathbf{e}_i parallel to \mathbf{m}_i , it can be shown that the velocity gradient is specified by the form:

$$\mathbf{L} = \mathbf{D} = \frac{\dot{a}}{a} \mathbf{e}_1 \otimes \mathbf{e}_1 + \frac{\dot{b}}{b} \mathbf{e}_2 \otimes \mathbf{e}_2 + \frac{\dot{c}}{c} \mathbf{e}_3 \otimes \mathbf{e}_3 \quad (11)$$

where the symbol \otimes denotes the tensor product between two vectors, and a, b, c represent the stretches of material line elements in the coordinate directions $\mathbf{e}_1, \mathbf{e}_2$ and \mathbf{e}_3 , respectively, with initial conditions:

$$a(0) = b(0) = c(0) = 1 \quad (12)$$

The antisymmetric part \mathbf{W} of the velocity gradient and consequently \mathbf{W}_p vanish in the case of uniaxial stress, resulting in

$$\mathbf{L}_p = \mathbf{D}_p \quad (13)$$

Then the corresponding constituents of the distortional vector \mathbf{m}_i may be represented by the forms:

$$m'_{33} = a_m^2, m'_{11} = m'_{22} = \frac{1}{a_m} \quad (14)$$

$$\mathbf{m}'_3 = a_m \mathbf{e}_3$$

$$\mathbf{m}'_1 = \frac{1}{\sqrt{a_m}} \mathbf{e}_1, \mathbf{m}'_2 = \frac{1}{\sqrt{a_m}} \mathbf{e}_2$$

where a_m is a function to be determined. The deviatoric part \mathbf{D}' of \mathbf{D} may be defined by the equation:

$$\mathbf{D}' = \mathbf{D} - \frac{1}{3} (\mathbf{D} \cdot \mathbf{I}) \mathbf{I} \quad (15)$$

Combination of equations (6), (7), (9), (10) and (11) gives:

$$\frac{\dot{J}_m}{J_m} = \text{tr} \mathbf{L}_m = \mathbf{D} \cdot \mathbf{I} \quad (16)$$

$$\dot{m}'_{ij} = 2(\mathbf{D}' - \mathbf{D}_p) \cdot (\mathbf{m}'_i \otimes \mathbf{m}'_j)$$

where (following Rubin) the dot product $\mathbf{A} \cdot \mathbf{B}$ between two

tensors denotes the usual scalar product when \mathbf{A}, \mathbf{B} are vectors, and it denotes the scalar $\text{tr}(\mathbf{A}\mathbf{B}^T)$ when \mathbf{A} and \mathbf{B} are second order tensors.

The associate flow rule which defines the symmetric part of the plastic velocity gradient \mathbf{D}_p has been written by Rubin as:

$$\mathbf{D}_p = \Gamma_p \bar{\mathbf{D}}_p \quad (17)$$

where the direction of $\bar{\mathbf{D}}_p$ for plastically isotropic response has the following form:

$$\bar{\mathbf{D}}_p = \frac{J_m}{2\mu} [\mathbf{T}' \cdot (\mathbf{m}'_i \otimes \mathbf{m}'_j)] \left(\mathbf{m}'_i \otimes \mathbf{m}'_j - \frac{1}{3} m'_{ij} \mathbf{I} \right) \quad (18)$$

where Γ_p is a non-negative function expressing the rate of plastic deformation and needs to be specified.

In order to completely formulate the set of constitutive equations, Rubin has used the hyperelastic formula for the developed stress. According to his procedure, the distortional vectors \mathbf{m}'_i are responsible for this calculation of the elastic response.

For the case of isotropic elastic response, the suitable equation for the deviatoric part of the developed stress \mathbf{T}' is:

$$\mathbf{T}' = \mu J_m^{-1} (\mathbf{m}'_r \otimes \mathbf{m}'_r - \frac{1}{3} m'_{rr} \mathbf{I}) \quad (19)$$

with μ being the shear modulus.

Semicrystalline polymers, however, which in the undeformed state are isotropic, start behaving anisotropically due to the alignment of microcrystalline regions under the imposed stress field. This anisotropic elastic response has been the subject of numerous theoretical works^{1,2} where various models for its detailed description have been introduced.

The most established and commonly used model which couples molecular structure with bulk properties for the mechanical behaviour at large deformations is the aggregate model¹⁶.

According to this model, a crystalline polymer is composed of two phases (crystalline and non-crystalline), each of them having its own unique structural elements. A fundamental assumption of this approach is that the constituent elements are identical during the deformation process. That is, although the test procedure may change the orientation of the unit cells, their size and elastic constants remain unaffected.

Furthermore, a unit cell is considered to be a transversely isotropic material, characterized by five elastic compliances s_{ij} . This type of anisotropy also concerns the macroscopic behaviour of the material.

In order to determine the mechanical properties of the deformed polymer, exact details of the molecular arrangement and microcrystalline orientation are necessary. The average elastic constants for the aggregate model can be obtained by two ways, either by assuming uniform stress through the aggregate (which implies a summation of compliance constants) or uniform strain (which implies a summation of stiffness constants). In our case, the first assumption (Reuss average)⁵ has been followed because it seems to fit better to the experimental results for a number of semicrystalline polymers^{1,16}.

The essential mathematical step for defining the compliances of the whole material, apart from the above assumptions, is the definition of the orientation of a single unit through the angle θ between its symmetry axis and the draw direction, and angle φ between the projection of a

symmetry axis on a plane perpendicular to the draw direction. By adopting the pseudo affine deformation scheme of Kuhn and Grun¹⁷, the angle θ changes to θ' as:

$$\tan \theta' = \frac{\tan \theta}{a^{3/2}} \quad (20)$$

where a is the stretch ratio in the draw direction.

By suitable integration in all directions, the elastic compliances¹⁶ are given by the following equations:

$$s'_{11} = \frac{1}{8}(3I_2 + 2I_5 + 3)s_{11} + \frac{1}{4}(3I_3 + I_4)s_{13} + \frac{3}{8}I_1s_{33} + \frac{1}{8}(3I_3 + I_4)s_{44} \quad (21)$$

$$s'_{12} = \frac{1}{8}(I_2 - 2I_5 + 1)s_{11} + I_5s_{12} + \frac{1}{4}(I_3 + 3I_4)s_{13} + \frac{1}{8}I_1s_{33} + \frac{1}{8}(I_3 - I_4)s_{44}$$

$$s'_{13} = \frac{1}{2}I_3s_{11} + \frac{1}{2}I_4s_{12} + \frac{1}{2}(I_1 + I_2 + I_5)s_{13} + \frac{1}{2}I_3s_{33} - \frac{1}{2}I_3s_{44}$$

$$s'_{33} = I_1s_{11} + I_2s_{33} + I_3(2s_{13} + s_{44})$$

$$s'_{44} = (2I_3 + I_4)s_{11} - I_4s_{12} - 4I_3s_{13} + 2I_3s_{33} + \frac{1}{2}(I_1 + I_2 - 2I_3 + I_5)s_{44}$$

The five independent elastic compliances s_{ij} of the unit cell, which characterize the crystalline phase of isotactic polypropylene, have been measured in a previous work¹⁸. The tests have been made at room temperature on fully extended films, which were considered to be transversely isotropic, at various directions in respect to the film draw direction, and were considered to have the same compliances of the unit cell. The values of these elastic constants s_{ij} used are taken from ref. ¹⁸, and are as follows: $s_{11} = 12$, $s_{33} = 1.6$, $s_{44} = 10$, $s_{13} = -0.73$, $s_{12} = -17 \times 10^{-10} \text{ m}^2\text{N}^{-1}$.

On the other hand, the terms I_1 , I_2 , I_3 , I_4 , I_5 are the orientation functions defining the average values of $\sin^4\theta$ (I_1), $\cos^4\theta$ (I_2), $\cos^2\theta \sin^2\theta$ (I_3), $\sin^2\theta$ (I_4), $\cos^2\theta$ (I_5) for the aggregate.

The orientation functions can be calculated on the pseudo-affine deformation scheme and then the aggregate model predicts the general form of the mechanical anisotropy.

For transversely isotropic materials, the general constitutive equation is:

$$\mathbf{E} = \mathbf{S}\mathbf{T} \quad (22)$$

where \mathbf{E} is the deformation strain tensor, \mathbf{T} is the stress tensor, both expressed in terms of a column matrix and \mathbf{S} is the compliance matrix given by:

$$\mathbf{S} = \begin{bmatrix} s'_{11} & s'_{12} & s'_{13} & 0 & 0 & 0 \\ s'_{12} & s'_{11} & s'_{13} & 0 & 0 & 0 \\ s'_{13} & s'_{13} & s'_{33} & 0 & 0 & 0 \\ 0 & 0 & 0 & s'_{44} & 0 & 0 \\ 0 & 0 & 0 & 0 & s'_{44} & 0 \\ 0 & 0 & 0 & 0 & 0 & 2(s'_{11} - s'_{12}) \end{bmatrix} \quad (23)$$

On the other hand, when the material is subjected to a uniform compressive stress field p , the dilatation J_m is given by:

$$p = [2(s'_{11} + s'_{12}) + 4s'_{13} + s'_{33}]^{-1} \left(\frac{1}{J_m} - 1 \right) \quad (24)$$

In the case of uniaxial tension, which is considered in this work, and taking into account that the deformation tensor is expressed in terms of vectors \mathbf{m}_i' , using the values of \mathbf{m}_i' in respect to equation (14), the deviatoric parts of implied stress tensor \mathbf{T}' take the form:

$$T'_{33} = \frac{2}{3} \frac{1}{J_m 2(s'_{33} - s'_{13})} \frac{a_m^3 - 1}{a_m} \quad (25)$$

and

$$T'_{11} = T'_{22} = \frac{-1}{3} \frac{1}{J_m 2(s'_{33} - s'_{13})} \frac{a_m^3 - 1}{a_m}$$

Since the lateral boundary is stress-free,

$$p = T'_{22} \quad (26)$$

which in respect to equations (24) and (25) gives:

$$J_m = 1 + \frac{2(s'_{11} + s'_{12}) + 4s'_{13} + s'_{33}}{6(s'_{33} - s'_{13})} \frac{a_m^3 - 1}{a_m} \quad (27)$$

By differentiating with respect to time:

$$\frac{\dot{J}_m}{3J_m} = \frac{2(s'_{11} + s'_{12}) + 4s'_{13} + s'_{33}}{1 + \frac{2(s'_{11} + s'_{12}) + 4s'_{13} + s'_{33}}{6(s'_{33} - s'_{13})} \frac{a_m^3 - 1}{a_m}} \frac{\dot{a}_m}{a_m} \quad (28)$$

On the other hand, the time evolution of dilatation J_m can be derived by combining equations (11) and (16) as:

$$\frac{\dot{a}}{a} = \frac{\dot{J}_m}{3J_m} + D'_{33}, \quad \frac{\dot{b}}{b} = \frac{\dot{J}_m}{3J_m} + D'_{11}, \quad \frac{\dot{c}}{c} = \frac{\dot{J}_m}{3J_m} + D'_{22} \quad (29)$$

where the deviatoric parts \mathbf{D} of the symmetric velocity gradient, following equations (16) and (29) are given by:

$$D'_{33} = \frac{\dot{a}_m}{a_m} + D_p 33 = \frac{\dot{a}_m}{a_m} + \frac{\Gamma_p a_m^3 - 1}{18 a_m^3} (4a_m^6 + 2) \quad (30)$$

$$D'_{11} = -\frac{1}{2} \frac{\dot{a}_m}{a_m} - D_p 11 = -\frac{1}{2} \frac{\dot{a}_m}{a_m} - \frac{\Gamma_p a_m^3 - 1}{18 a_m^3} (2a_m^6 + 1)$$

$$D'_{22} = -\frac{1}{2} \frac{\dot{a}_m}{a_m} - D_p 22 = -\frac{1}{2} \frac{\dot{a}_m}{a_m} - \frac{\Gamma_p a_m^3 - 1}{18 a_m^3} (2a_m^6 + 1)$$

Substituting equations (30) into equations (29) we obtain the time evolution of the stretch ratio a_m ,

$$\frac{\dot{a}_m}{a_m} = \frac{1 + \frac{2(s'_{11} + s'_{12}) + 4s'_{13} + s'_{33}}{6(s'_{33} - s'_{13})} \left(\frac{a_m^3 - 1}{a_m} \right)}{1 + \frac{2(s'_{11} + s'_{12}) + 4s'_{13} + s'_{33}}{18(s'_{33} - s'_{13})} \left(\frac{5a_m^3 - 2}{a_m} \right)} \times \left[\frac{\dot{a}}{a} - \frac{\Gamma_p}{18} \left(\frac{a_m^3 - 1}{a_m^3} \right) (4a_m^6 + 2) \right] \quad (31)$$

with the initial condition $a_m(0) = 1$. The functional form of Γ_p has been mentioned in the previous section and expressed by equation (2). The amplification factor k of equation (2) is considered to be strain rate and state of

deformation independent. Consequently, k can be evaluated at the stage where yield initiates and the stretch ratio a_m is approximately equal to 1, while \dot{a}_m is almost equal to zero. Using these approximations in equation (31) we obtain:

$$\Gamma_p \cong \frac{\dot{a}}{a a_m - 1} \quad (32)$$

At the reference zone, \dot{a} is equal to $\dot{\epsilon}_r$, and the coefficient k is equal to $1/[a(a_m - 1)]$ or equal to $1/(a\epsilon_{el})$ where ϵ_{el} is the elastic strain of this zone, and $a \cong 1.12$, as is shown in the experimental data of Figure 7. At the yield point ϵ_{el} can be approximated as σ_y/E , where E is the modulus. Therefore, the factor k is given by:

$$k = \frac{E}{\sigma_y a} \cong \frac{1250(\text{MPa})}{301.12(\text{MPa})} \cong 37.2 \quad (33)$$

The integration of equation 31 determines the value of stretch ratio a_m at every state of elongation, leading to the calculation of the imposed stress for the elastic plastic response.

The integration method has been made numerically, using small time steps, with the software 'Mathematica'¹⁹ and a personal computer. Decreasing gradually the original time step up to one tenth, a high convergence has been obtained.

The isovolume plastic deformation of these materials has been testified by examining the numerical values of the dilatation J_m . It has been found that J_m after yielding is almost equal to unity. The solution of the system of the above equations is presented in Figure 8 for a strain rate of 1 mm/min, in terms of curve (a). In the same plot, curve (b) shows the solution of the same system where the evolving anisotropy is not taken into account and the elastic response is calculated from the initial values of the elastic compliances s_{ij} . Although the difference between these two curves is appreciable, the contribution of the crystalline orientation to the s_{ij} values through the orientation functions of equation (21) does not describe totally the experimentally observed strain hardening.

This inadequacy may be due to the type of the orientation function used through the pseudoaffine deformation resulting in equation (20). A stronger dependence from the stretch ratio probably could accommodate accurately the evolving anisotropy of the elastic response. Another way, however, to describe the strain hardening after yield, which is observed in the true stress-strain curves, is to introduce an additional term in the constitutive equation which is known as entropic hardening^{10,11}.

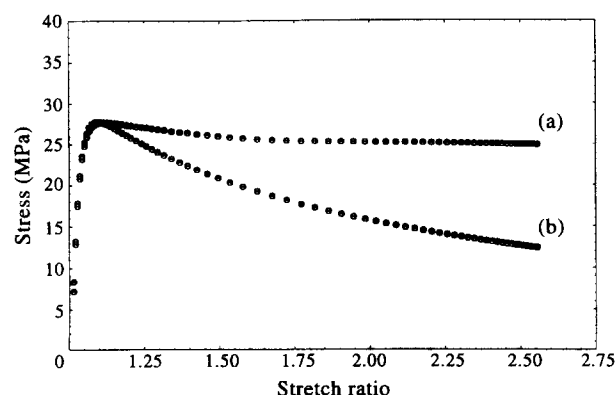


Figure 8 Theoretical tensile stress-strain curve of polypropylene, at a cross-head speed of 0.1 mm/min, obtained from the solution of the system of constitutive equations. Curve (a): with elastic compliances varying with draw ratio. Curve (b): with constant elastic compliances

The entropic hardening term can be represented as a stress based on the theory of rubber elasticity¹¹. The modelling of entropic resistance has also been reported by Parks et al.²⁰. Upon stretching, the chains begin to orient in an affine manner and this effect can be described by the statistical mechanics network models of rubber elasticity⁹. In our case, the three-chain model of James and Guth²¹ has been used. In this way, the principal components T_{ii}^* of the measured stress may be expressed as:

$$T_{ii}^* = T_{ii} + B_{ii} \quad (34)$$

where T_{ii} is the principal stress obtained from the constitutive equations and B_{ii} is given by:

$$B_{ii} = G_p \frac{\sqrt{N}}{3} \left[a_i L^{-1} \left(\frac{a_i}{\sqrt{N}} \right) - \frac{1}{3} \sum_{j=1}^3 a_j L^{-1} \left(\frac{a_j}{\sqrt{N}} \right) \right] \quad (35)$$

where a_i is the stretch ratio, N is the number of rigid links between entanglements. As is mentioned by Boyce et al.¹⁰ \sqrt{N} is equal to the terminal or locking stretch. From the true stress-strain curves of Figure 7, it is shown that locking occurs at a ratio almost equal to 3, resulting in a value for N approximately equal to 9. G_p is the strain hardening modulus which can be calculated by differentiating equation (34) with respect to a at the position of yield initiation. Therefore, with N equal to 9 and by differentiating at $a = 1.12$, where T_{ii} is equal to Y (the yield stress) we have:

$$\frac{Y}{G_p} \geq 2.46 \quad (36)$$

At the lower cross-head speed, Y is equal to 25 MPa, so from equation (36) it is obtained that $G_p \leq 10$. By adding this term into the above mentioned constitutive equation, the whole true stress-strain curve can be described.

The constitutive equations, as presented above, including the strain hardening effect, do not predict, however, the rate effect commonly observed in polymeric materials and being obvious in the experimental stress-strain curves. This phenomenon, directly related to molecular relaxation processes, is determined from the early stage of deformation and should be incorporated in the above constitutive equations, in order to have a detailed description of the yield behaviour.

At small deformations, before yielding, the semicrystalline polymer is still isotropic and the material response can be simply described in terms of scaling rule, valid in the viscoplasticity. Such scaling rules, commonly used in the literature, have also been applied for glassy polymeric

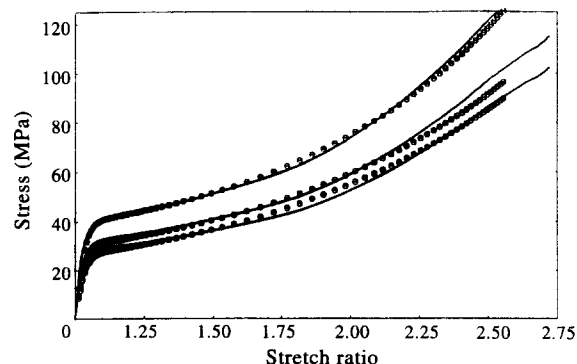


Figure 9 Tensile true stress-strain curves on polypropylene: theoretical results versus experimental data

materials by Matsuoka²². According to this rule, a stress-strain curve at a strain rate $\dot{\epsilon}_2$ can be predicted from an experimental curve obtained at a rate $\dot{\epsilon}_1$ by multiplying the stress in the experimental curve by the scaling factor $(\dot{\epsilon}_2/\dot{\epsilon}_1)^n$. The power coefficient n is directly connected with the relaxation mechanism for macromolecules and is found to be equal to 0.06 for describing the experimental data of our work.

Taking all these effects into account, the stress-strain curves evaluated from the solution of the system of constitutive equations are plotted in Figure 9, where a very accurate prediction of the experimental results in the three cross-head speeds examined is shown.

CONCLUSIONS

The inhomogeneous plastic deformation, i.e. the neck initiation and its propagation, which is abounded in semicrystalline polymers, strongly affects the obtained stress-strain curve. The construction of the true stress-strain plot requires particular experimental techniques. In this work, a new non-contact method with a Laser extensometer has been used. By this technique, a pattern code is applied on the specimen dividing its gauge length into zones each of 1 mm width. The reflections of the laser beam of each zone provide the strain and the subsequent strain rate separately, resulting in deformation distribution across the specimen. The strain rate of the localized plastic region was then able to be measured, and was found to differ about two orders of magnitude in respect to the imposed cross-head speed.

In order to obtain the rate of plastic deformation, a scaling rule has been postulated from the experimental results, as shown in Figure 5. The evaluation of this magnitude permits the constitutive description of the plastic formulation developed by Rubin for the case of soft crystalline metals.

This formulation has the advantage, with respect to other plasticity theories, to describe in detail the inhomogeneous deformation through the velocity gradient tensor \mathbf{L} . This is due to the fact that for inhomogeneous deformation, the deformation gradient tensors of elastic and plastic part \mathbf{F}_e and \mathbf{F}_p , respectively, are not integrable in the displacement field, whereas the total deformation gradient tensor \mathbf{F} is always integrable. Using the described formulation, the numerical integration of the constitutive equations predicts exactly the yield behaviour.

In order to incorporate the strain hardening effect which appears after yielding, we complete the above analysis by

using the entropic hardening terms, as has been previously done by other authors.

Finally, the rate effect of yielding, usually observed in polymeric materials, has been described with a scaling rule of non-linear viscoelasticity.

The elastic compliances used in this description are constants of the transversely isotropic crystalline phase of polypropylene established in the literature. The remaining parameters used in the calculations were identified as material constants.

The above treatment can be applied in every type of semicrystalline, cold drawing materials and consists of a general description for elastically anisotropic, plastically isotropic materials.

REFERENCES

1. Samuels, R. J., *Jnl. Polym. Sci.*, 1972, A-2, **10**, 781.
2. Seferis, J. C. and Samuels, R. J., *Polym. Eng. Sci.*, 1979, **19**, 975.
3. Ward, I. M., *Proc. Phys. Soc.*, 1962, **80**, 1176.
4. Kausch, H. H., *Kolloidzeitschrift*, 1970, **237**, 251.
5. Reuss, A., *Zeit. Angew. Math. Mech.*, 1929, **9**, 49.
6. Voigt, W., *Lehrbuch der Kristallphysik*, Teubner, Leipzig, 1928, p.410.
7. Sawczuk, A. and Bianchi, G., *Plasticity Today*, Elsevier Applied Science, 1985.
8. Duffo, P., Monasse, B., Haudin, J. M., Sell, C. G. and Dahoun, A., *Journal of Material Science*, 1995, **30**, 701.
9. Treloar, L. R. G., *The Physics of Rubber Elasticity*, Clarendon Press, Oxford, 1975.
10. Boyce, M. C., Parks, D. M. and Argon, A. S., *Mechanics of Materials*, 1988, **7**, 15-33.
11. Haward, R. N., *Journal of Polymer Science, Part B*, 1995, **33**, 1481.
12. Rubin, M. B., *Plasticity theory formulated in terms of physically based microstructural variables—Part I. Theory. Journal of Solids and Structures*, 1994, **31**(19), 2615.
13. Rubin, M. B., *Plasticity theory formulated in terms of physically based microstructural variables—Part II. Examples. Journal of Solids and Structures*, 1994, **31**(19), 2635.
14. Eckard, C., *Phys. Rev.*, 1948, **73**, 373.
15. Besseling, J. F., *Proc. IUTAM Symp. on Irreversible Aspects of Continuum Mechanics*, Vienna, pp.16-53, Springer, 1968.
16. Ward, I. M., *Mechanical Properties of Solid Polymers*, John Wiley, 1983.
17. Kuhn, W. and Grun, F., *Kolloidzeitschrift*, 1942, **101**, 248.
18. Hadley, D. W., Pinnock, P. R. and Ward, I. M., *Journal of Material Science*, 1969, **4**, 152.
19. Wolfram, S., *Mathematica, A System for Doing Mathematics by Computer*, Second Edition, Wolfram Research, 1993.
20. Parks, D. M., Argon, A. S. and Bagepalli, B., MIT Program in Polymer Science and Technology Report, Massachusetts Institute of Technology, 1984.
21. James, H. M. and Guth, E., *J. Chem. Phys.*, 1943, **11**, 455.
22. Matsuoka, S., *Relaxation Phenomena in Polymers*, Second Edition, Hanser, 1992, ch.3.